(7) Hayashi, K.; Yamamoto, Y.; Miki, M. *Proc. 6th Int. Radiat. Conf.* **1979**, 385.
(8) Hayashi, K.; Yamamoto, Y.; Miki, M. *Macromolecules* **1976**, *9*, 874.
(9) Hayashi, K.; Yamamoto, Y.; Miki, M. *Macromolecules* **1977**, *10*, 1316.
(10) Ito, H.; Willson, C. G.; Frechet, J. M. J. *Macromolecules* **1983**, *16*, 510.
(11) Klein, A. Ger Offen. 2356813, 1975.
(12) Klein, A. Ger Offen. 2304588, 1974.
(13) Olah, G. A.; Schleyer, P. *Carbonium Ions*, Wiley-Interscience: New York, 1970; Vol. II, p 488.

Coil-Stretch Transitions in Mixed Shear and Extensional Flows of Dilute Polymer Solutions

R. G. Larson* and J. J. Magda†

AT&T Bell Laboratories, 600 Mountain Avenue, Murray Hill, New Jersey 07974-2070.
Received December 6, 1988

ABSTRACT: A generalization of Zimm's bead-spring model for dilute solutions of flexible polymers that accounts for the influence of coil distortion on hydrodynamic interactions is used to calculate molecular distortions and coil-stretch transitions in general planar flows. Expressing an arbitrary incompressible planar flow as a superposition of a shearing flow and a planar extension, we find that the shearing flow can reduce the critical extension rate $\dot{\epsilon}_c$ required to produce a coil-stretch transition, whereas the original Zimm theory predicts no influence of shearing on $\dot{\epsilon}_c$. The scaling theory of de Gennes predicts a much larger influence of shearing on $\dot{\epsilon}_c$ than is obtained in the bead-spring calculations, apparently because the cylindrical shape assumed by de Gennes does not accurately describe the true pretransition coil shape. The weaker dependence of $\dot{\epsilon}_c$ on shearing found in our calculations is consistent with recent experimental data of Dunlap and Leal.

I. Introduction

Understanding and prediction of the rheological properties of flexible or rigid polymers in dilute solution are of considerable importance, not only because of the technological uses of such polymers as drag-reducing agents or viscosity builders but also because the dilute solution properties can be used to infer molecular structural information such as molecular weight and flexibility. Since the dilute regime of polymer solutions is characterized by the absence of intermolecular interactions, one might suppose that the rheological properties in the dilute regime ought to be easily understood, at least in comparison to concentrated solutions. Although this seems to be true of rigid molecules, understanding of the dilute-solution properties of flexible polymers is still sketchy except in the small deformation regime of linear viscoelasticity. Though it has been known for at least 50 years, for example, that shear thinning occurs when dilute solutions are sheared at high rates, the causes of shear thinning are still not known with confidence.[1]

There are several reasons that the viscoelastic properties of dilute solutions of flexible polymers, despite their seeming simplicity, have been difficult to understand or predict. First, although the chains do not interact with each other, there are *hydrodynamic interactions* between different parts of the same chain.[2] The solvent velocity and hence the drag forces near one part of the chain are influenced by the drag forces acting on other parts of the same chain. The strength of the hydrodynamic interaction between two segments of the chain depends on the separation between the two segments and thus on the chain conformation. Only in the limit of small chain deformation—that is, in the linear viscoelastic limit—is the distribution of chain conformations known a priori. At modest or high deformation rates, the chain conformation distribution and the hydrodynamic interactions are coupled and solution of the coupled problem is difficult unless drastic approximations are made.

A second hurdle impeding understanding of dilute solution rheology is the effect of excluded volume and solvent-polymer interactions on chain conformation in the presence of a strongly distoring flow field. Only in special Θ conditions can this effect truly be neglected.[2]

Despite these and other difficulties, some important qualitative insight has been developed, especially in extensional flows. In particular, it has been recognized for many years that a polymer coil in an extensional flow at strain rates above a critical value undergoes a coil-to-stretch transition in which the molecule unravels to a nearly fully extended state.

More recently it has been appreciated that hydrodynamic interaction can increase the abruptness of this transition. As the polymer molecule is stretched in an extensional flow, hydrodynamic interactions between different parts of the molecule are weakened, thus changing the effective drag force exerted by the solvent on the polymer. Because of hydrodynamic interaction, in the undistorted or nearly undistorted state the drag the solvent exerts on a polymer molecule of high molecular weight is equivalent to the drag that would be exerted on an impenetrable sphere having an effective radius comparable to the radius of gyration of the polymer molecule. This is the so-called "nondraining" picture of the polymer coil. de Gennes[3] and Hinch[4] have extended this picture to the highly distorted state, modeling the deformed polymer as an effective impenetrable cylinder. As the cylinder is extended in an extensional flow, its surface area, and therefore the drag exerted on it by the solvent, increases in proportion to its length. If the distortion of the molecule were to become so severe that hydrodynamic interactions were rendered negligible, then the polymer molecule could be considered a "freely draining" object in which the drag on each portion of the molecule is unaffected by the drag on other portions. The nondraining and freely draining limits are also called the Zimm[5] and Rouse[6] limits, respectively.

de Gennes suggested a simple elastic dumbbell model for the polymer molecule. The dumbbell is characterized

† Department of Chemical Engineering, University of Utah, Salt Lake City, UT 84112.

0024-9297/89/2222-3004$01.50/0

by a relaxation time τ that is proportional to the effective drag coefficient of the polymer in the solvent. According to the cylinder picture, τ should increase in rough proportionality to the end-to-end length R of the dumbbell, until a saturation value τ^R, the Rouse relaxation time, is reached. de Gennes represented this behavior by the simple expression

$$\tau = \frac{\tau^R}{1 + \beta/R} \tag{1}$$

Since the end-to-end length of the dumbbell is a stochastic quantity, we replace R by $\langle R^2\rangle^{1/2}$, where $\langle R^2\rangle$ is the mean square of the dumbbell end-to-end vector. This step, called the preaveraging approximation, uncouples the fluctuations in hydrodynamic interaction—and therefore in τ—from the fluctuations in chain extension R. In this approximation

$$\tau \approx \frac{\tau^R}{1 + \beta/\langle R^2\rangle^{1/2}} \tag{2}$$

When there is no deformation $\langle R^2\rangle = \langle R^2\rangle_0$, its equilibrium value. In this limit τ must equal τ^Z, the Zimm relaxation time. From this requirement β is found to be

$$\beta = \left(\frac{\tau^R}{\tau^Z} - 1\right)\langle R^2\rangle_0^{1/2} \tag{3}$$

τ^R/τ^T scales as the square root of the polymer molecular weight. Thus for high polymers τ^R/τ^Z is large (greater than 10 or so). For high polymers the formula

$$\tau = \tau^Z(\langle R^2\rangle/\langle R^2\rangle_0)^{1/2} \tag{4}$$

is almost equivalent to eq 2 except at high molecular extensions.

With this simple dumbbell model, one finds that the coil-to-stretch transition is abrupt; i.e., at a critical value of the dimensionless extension rate $\tau^Z\dot{\epsilon} = 0.275$ in planar extension the molecule is suddenly extended from a dimensionless length $(\langle R^2\rangle/\langle R^2\rangle_0)^{1/2} = (1 + {}^1/_3(6^{1/2}))^{1/2} \doteq 1.35$ to its fully extended length. (The extension rate $\dot{\epsilon}$ is just the velocity gradient in the direction of stretch; see section III.) This prediction of de Gennes's dumbbell model is not expected to be quantitatively correct, however, because the modest distortion predicted for the dumbbell just below the critical extension rate is not consistent with the long cylindrical shape assumed in the estimation of the relaxation time, eq 1. In shearing flows, the de Gennes dumbbell model predicts that near the shear rate $\tau^Z\dot{\gamma} = (3/2)^{1/2}$ the dumbbell will extend rapidly with small increases in $\dot{\gamma}$ until the distortion $(\langle R^2\rangle/\langle R^2\rangle_0)^{1/2}$ approaches the value τ^R/τ^Z. This result leads to a prediction of shear thickening at modest values of the shear rate that is at odds with experimental data.[7,8]

The experimental data of Fuller and Leal[9] and of Dunlap and Leal[10] in mixed shearing and extensional flows also conflict with the simple de Gennes dumbbell model. As discussed in detail in section IV, Leal and co-workers found that in mixed shear and planar extensional flows, the coil-to-stretch transition is controlled by the extensional component of the flow, even if the shearing flow is by far the dominant contribution to the total velocity gradient. The de Gennes dumbbell model predicts a significant effect of shear on the critical condition when the contribution of shear becomes comparable to that of the extensional flow. Leal and co-workers found better quantitative agreement of the dumbbell model with their data if the weakening of hydrodynamic interaction with polymer deformation is ignored, that is, if τ is kept constant at the Zimm value τ^Z. In this simpler model, which we shall call the Zimm dumbbell model, the coil-to-stretch transition occurs over a narrow but finite range of extension rates, and the transition is complete when $\tau^Z\dot{\epsilon}$ reaches the value ${}^1/_2$.

II. Bead-Spring Chains

An improved theory of hydrodynamic interaction in dilute polymer flows is afforded by the bead–spring model, from which Zimm[5] in 1956 computed viscoelastic properties in the limit of small deformations. In this model, many beads and springs are connected in series. The springs account for a Gaussian elastic force in the polymer and the drag force—that is really distributed continuously along the chain—is concentrated at a finite but large number of discrete beads.

The basic rationale for the bead–spring model is as follows. As the molecular weight increases with solvent quality held fixed, the rheological behavior of a flexible polymer ought to approach an asymptotic limit in which the behavior becomes independent of the details of the local chemical structure of the chain apart from numerical prefactors. Likewise as the number of beads and springs in an idealized bead–spring chain increases, its behavior approaches an asymptotic limit, and this limit ought to match that of the real chain, if the asymptotic behavior of the real chain really is independent of local chain structure.

The good agreement between Zimm's bead–spring theory and experimental linear viscoelastic data[2] suggests that the basic idea is sound. It would thereore be worthwhile to extend the theory to the regime of nonlinear viscoelasticity. Since polymers of high molecular weight must be highly distorted before non-Gaussian elastic effects are expected to be important, there ought to be a regime of modest distortions beyond the linear regime in which the bead–spring description remains valid. The higher the molecular weight of the molecule, the more it can be distorted before it fails to behave as an asymptotically long molecule. Thus the magnitude of polymer distortion at which the bead–spring model breaks down should increase with molecular weight, and one can estimate that distorted coils that have been stretched by a factor of 10 should still be well described by a bead–spring model if the molecular weight is in the hundreds of thousands. If the molecular weight is in the millions or tens of millions, stretch ratios of up to 100 could conceivably be described by the bead–spring model. (If the transient strain rate is very high or if the rate of chain distortion is high, however, then the bead–spring model is expected to fail even before the chain becomes so highly distorted that non-Gaussian elastic forces come into play. Thus if the rate of chain stretching is faster than the rate at which a portion of the real chain represented by a single spring can sample its distribution of configurations, then this portion cannot be considered an entropic spring—either Gaussian or non-Gaussion—and the bead–spring model is not appropriate. Bead–spring models also do not account for noncrossability conditions or self-entanglements; the chain is assumed to contain phantom springs that can pass through each other. Although self-entanglements are probably not important in steady-state extensional flow, their significance in steady-state shear or mixed flows is uncertain.)

With this motivation, Fixman[11] in 1966 extended Zimm's technique, allowing calculation of the effects of hydrodynamic interaction and excluded volume when the chains experience modest levels of distortion. Fixman's calculations for the shear viscosity of a dilute polymer solutions under Θ conditions seem to agree with the most reliable experimental data. Öttinger,[12] employing a somewhat

different (and much more computationally intensive) technique, could do similar calculations. The primary approximation in both Fixman's and Öttinger's methods is preaveraging of the hydrodynamic drag tensors. Zimm had also employed preaveraging, but he preaveraged over the *equilibrium* distribution of polymer configurations, while Fixman and Öttinger preaveraged over the distorted distribution. In Fixman's technique, Zimm's solution for the second moment of the distribution function was used to preaverage the drag tensors, and these preaveraged tensors were used to compute a more accurate second moment of the distribution function as well as the stress. Thus Zimm's technique can be regarded as a first-order perturbation about the rest state and Fixman's a second-order perturbation. Öttinger continued the iterative procedure until consistency was achieved between the computed moment and that used to preaverage the drag tensors. In recent calculations of Magda et al.,[13] the Fixman technique (which is much faster computationally than Öttinger's), was upgraded to achieve consistency between the preaveraged drag tensors and the moment of the distribution function. This upgraded Fixman technique was found to give results virtually identical with those obtained by Öttinger in shear flow with 25 beads (the maximum considered by Öttinger), but at a small fraction of the computer time.

With the upgraded Fixman technique, properties can now be computed for chains containing hundreds of beads. This is important, since only when the number of beads and springs is asymptotically large can we expect the behavior of the bead–spring chain to be comparable to that of real high molecular weight polymers. Other than the idealization of a Gaussian bead–spring model of a flexible polymer, the most important approximation in the upgraded Fixman technique is preaveraging. Using molecular dynamics calculations, Fixman[14] found that preaveraging introduces errors of 5–10% in the zero-shear viscosity. In the nonlinear regime, the magnitude of error introduced by preaveragng is as yet not known.

In the work of Magda et al. the upgraded Fixman technique was used to compute the uniaxial extensional viscosity of a dilute polymer solution under Θ conditions. A sharp coil-to-stretch transition was found at a critical extension rate $\dot{\epsilon}_c\tau^Z = 0.5035$, a value 7% *higher* than the critical strain rate of the Zimm dumbbell. (For the bead–spring chain we define τ^Z to be the longest relaxation time in the Zimm approximation.) $\dot{\epsilon}_c$ is increased relative to the Zimm dumbbell, because for the bead–spring chain the longest relaxation time τ at first decreases when the molecule is distorted from equilibrium and increases only after significant distortion occurs. The same nonmonotonic dependence of τ on chain distortion occurs in shearing flow and produces shear *thinning* at modest shear rates (in agreement with experiments), followed by shear thickening at high rates of shear. In the de Gennes dumbbell model the relaxation time increases monotonically with coil distortion and thus the critical extension rate $\dot{\epsilon}_c\tau^Z$ must be less than the Zimm value of 0.5. For the same reason, the de Gennes model predicts only shear thickening and no shear thinning in shearing flows. Given that de Gennes' model approximates the hydrodynamic interaction by treating the polymer molecule as a long cylinder, it is not surprising that it is inaccurate when coil distortions are modest.

In the present work, the upgraded Fixman technique is applied to general steady incompressible planar flows, which in section III are shown to be mixtures of shear and planar extension. We then find in section IV that the shearing component of the flow changes the critical extension rate $\dot{\epsilon}_c$ for a coil-to-stretch transition but by far less than the de Gennes model predicts. We show in section V that if the dependence of the relaxation on the chain distortion assumed in de Gennes' dumbbell model is corrected in light of our findings with the bead–spring chain, the qualitative behavior of the complex bead–spring chain in mixed flows can be reproduced by the dumbbell model. Finally it is argued that this simple correction to the dumbbell model should reduce or eliminate discrepancies between model predictions and experimental data, such as the data of Dunlap and Leal.

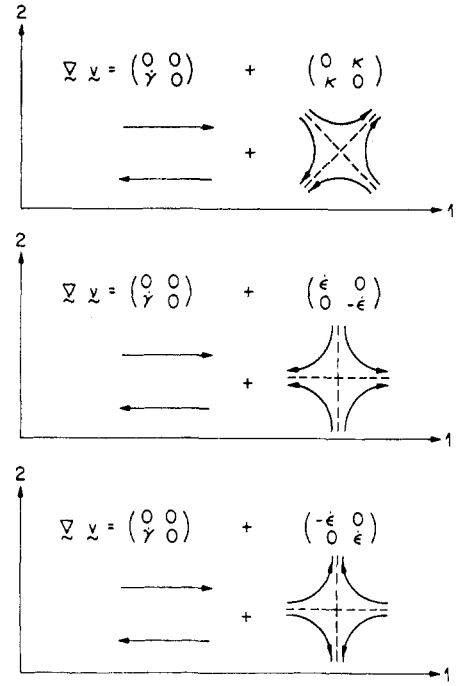

Figure 1. Decompositions of incompressible planar flows into superpositions of shear and extensional flows.

III. Kinematics and Stress Invariants

For a general incompressible planar flow, the velocity gradient tensor can be expressed in several equivalent ways. Fuller and Leal[9] expressed it as

$$\nabla\mathbf{v} = \frac{1}{2}G\begin{pmatrix} 1+\rho & -(1-\rho) \\ (1+\rho) & -(1-\rho) \end{pmatrix} \tag{5}$$

where G is a parameter controlling the overall magnitude of $\nabla\mathbf{v}$ and ρ controls the flow type. $\rho = 1$ corresponds to a planar extensional flow, $\rho = 0$ is simple shear, and $\rho = -1$ is pure rotation.

If this flow field is rotated 45°, the velocity gradient takes the following form used by de Gennes:[3]

$$\nabla\mathbf{v} = \begin{pmatrix} 0 & \kappa \\ \dot{\gamma}+\kappa & 0 \end{pmatrix} \tag{6}$$

where $\kappa = G\rho$ and $\dot{\gamma} = G(1-\rho)$. In this form, the flow field can be visualized as a superposition of a simple shear with shear rate $\dot{\gamma}$ and a planar extension with extension rate κ; see Figure 1 (top). The shear flow is oriented such that direction "1" is the flow direction and direction "2" is the gradient direction; the planar extension is oriented such that the stretch direction is at a 45° angle between directions 1 and 2. At this orientation, the extensional flow enhances the stretching produced along the 45° line by the shearing flow.

If $\dot{\gamma}$ and $\kappa + \dot{\gamma}$ are of the same sign (i.e., $\rho \geq 0$), then a further rotation of the flow field through an angle θ, with

$\sin\theta = -(\kappa/(2\kappa + \dot{\gamma}))^{1/2}$, produces

$$\nabla v = \begin{pmatrix} \dot{\epsilon} & 0 \\ \dot{\gamma} & -\dot{\epsilon} \end{pmatrix} \tag{7}$$

Here $\dot{\epsilon} = (\kappa(\dot{\gamma} + \kappa))^{1/2} = G\rho^{1/2}$ and the values of $\dot{\gamma}$ in eq 6 and 7 are numerically the same. A simple way to produce this velocity gradient is to superpose a planar extension with strain rate $\dot{\epsilon}$ in direction 1 onto a shearing flow with strain rate $\dot{\gamma}$. In the shearing flow, direction 1 is the flow direction and direction 2 is the gradient direction; see Figure 1 (middle).

If the velocity gradient in eq 6 is instead rotated through an angle θ with $\sin\theta = (\kappa(2\kappa + \dot{\gamma}))^{1/2}$, the result is

$$\nabla v = \begin{pmatrix} -\dot{\epsilon} & 0 \\ \dot{\gamma} & \dot{\epsilon} \end{pmatrix} \tag{8}$$

with $\dot{\epsilon}$ again given by $(\kappa(\kappa + \dot{\gamma}))^{1/2}$. Here the extensional flow is superposed with the stretching direction in direction 2—i.e., in the direction of the gradient of velocity; see Figure 1 (bottom). Thus, except for a trivial rotation of frame, the same velocity gradient is obtained when the extensional flow is superposed with the stretching in the direction of shear flow as is obtained when the stretching is in the direction of the shear gradient.

The polymer contribution to the two-dimensional stress tensor

$$\sigma = \begin{pmatrix} \sigma_{11} & \sigma_{12} \\ \sigma_{12} & \sigma_{22} \end{pmatrix} \tag{9}$$

can be computed from the second moment of the distribution function

$$\sigma = \nu kT \sum_{i=1}^{N} \left[\frac{3}{b^2} \langle \mathbf{R}_i \mathbf{R}_i \rangle - \delta \right] \tag{10}$$

where ν is the number of molecules per unit volume and N is the number of springs in the bead–spring chain. For the Gaussian dumbbell, $N = 1$. $\mathbf{R}_i$ is the end-to-end vector of the ith spring. b^2 is the mean-square end-to-end vector of a single spring at equilibrium.

The two-dimensional invariants of this stress tensor are

$$\mathrm{tr}\ \sigma \equiv \sigma_{11} + \sigma_{22} \tag{11}$$

and

$$\det \sigma = \sigma_{11}\sigma_{22} - \sigma_{12}^2 \tag{12}$$

For our purposes the most relevant invariant is a combination of these:

$$\Delta\sigma \equiv (\nu k_B T)^{-1}[(\mathrm{tr}\ \sigma)^2 - 4 \det \sigma]^{1/2} \tag{13}$$

In planar extensional flow $\nu kT\ \Delta\sigma/\dot{\epsilon}$ is the extensional viscosity. In simple shear $(\Delta\sigma)^2 = N^2 + 4\sigma_{12}^2$ is a linear combination of the square of the first normal stress difference N_1 and the square of the polymeric contribution to the shear stress. $\Delta\sigma$ is also proportional to the polymer contribution to the intrinsic birefringence Δn of the flowing solution.

The Zimm dumbbell model predicts that the coil–stretch transition occurs at the strain rate

$$\dot{\epsilon}_c = [\kappa(\kappa + \dot{\gamma})]^{1/2} = G\rho^{1/2} = 1/2\tau^Z \tag{14}$$

Thus in the decompositions of ∇v given by eq 7 and 8, the critical extension rate $\dot{\epsilon}_c$ is independent of the superposed shear rate $\dot{\gamma}$. For the de Gennes dumbbell model with τ given by eq 4, $\dot{\epsilon}_c$ drops precipitously as $\tau^Z\dot{\gamma}$ approaches the value $(3/2)^{1/2}$. In this respect the Zimm dumbbell is in much better agreement with the data of Dunlap and Leal than is the de Gennes dumbbell model.

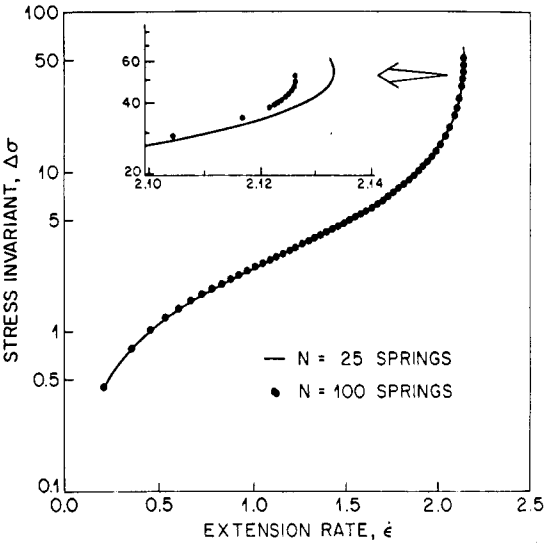

Figure 2. Stress invariant $\Delta\sigma$ versus extension rate for chains of 25 and 100 springs.

IV. Computational Results

The computer algorithm used in this work in described in ref 14. The few changes required for mixed flows are described in the Appendix. Θ conditions are assumed. The Zimm relaxation time τ^Z is nearly independent of the number of springs N and in dimensionless form is given by $1/\tau^Z = 4.066$. All quantities with units of time are here made dimensionless by mutliplying them by the characteristic frequency (see ref 14):

$$\lambda_0 \equiv 24k_BT[\eta_0 N^{3/2} b^3 (12\pi^3)^{1/2}]^{-1} \tag{15}$$

Figure 2 shows the stress invariant $\Delta\sigma$ versus the extension rate $\dot{\epsilon}$ in planar extension for the bead–spring chain with $N = 25$ and $N = 100$ springs. There is a turning point at a critical extension rate $\dot{\epsilon}_c = 2.133$; 5% higher than the critical Zimm value, 2.033. For extension rates exceeding $\dot{\epsilon}_c$, we expect the coil to unravel to a nearly fully extended state. The unraveling process itself is rapid and cannot be described by our bead–spring model, although we expect our calculations to be valid for steady extensional flows at extension rates up to $\dot{\epsilon}_c$, if the polymer molecular weight is high enough.

The experimental coil–stretch transition may occur at a strain rate slightly smaller than $\dot{\epsilon}_c$, because of the effect of *fluctuations in hydrodynamic drag*. If the extension rate is slightly less than $\dot{\epsilon}_c$, then fluctuations that increase the coil dimensions also increase hydrodynamic drag and can therefore induce the coil-to-stretch transition. These fluctuation effects are not accounted for in our calculations, since we have preaveraged the hydrodynamic drag tensor, thereby uncoupling fluctuations in drag from fluctuations in coil dimension. The extent to which hydrodynamic fluctuations reduce the coil-to-stretch strain rate depends on how long the coil resides in a extensional flow field at a given strain rate, but it can be estimated[3] that unless the residence time is of astronomical magnitude, the reduction in the coil-to-stretch strain rate produced by hydrodynamic fluctuations should be slight.

The coil dimension relative to its equilibrium value in each direction i in extensional flow at $\dot{\epsilon}_c$ can be obtained from[15]

$$\frac{\langle R_i^2 \rangle}{\langle R_i^2 \rangle_0} = 1 + 2\sum_{m=1}^{N} \left(\frac{\sin(m\pi/N + 1)}{1 - \cos(m\pi/N + 1)} \right)^2 \frac{\sigma_{ii}^m}{\nu k_B T} \tag{16}$$

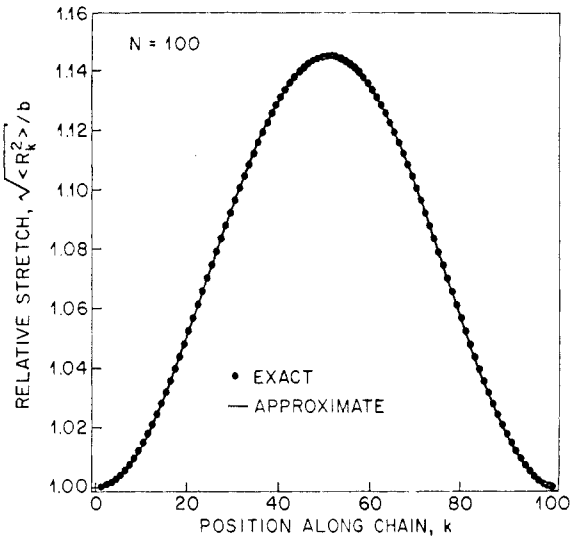

Figure 3. Length of stretched spring relative to its equilibrium length as a function of position along a 100-spring chain. The symbols are for the exact equation (18) and the line gives the approximate result, eq 19.

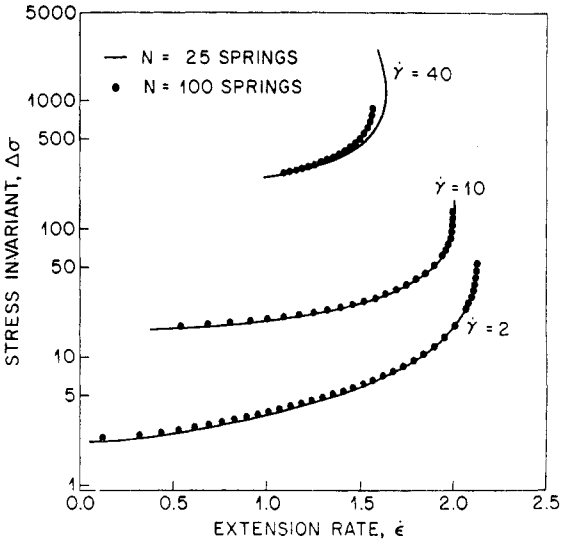

Figure 4. Stress invariant $\Delta\sigma$ versus extension rate for various fixed levels of shear as calculated from the bead–spring model. The velocity gradient tensor is given by eq 7.

Here σ_{ii}^m is the ii component of the contribution of mode m to the stress tensor. The slowest mode dominates the polymer coil behavior at $\dot{\epsilon}_c$; therefore one can approximate the above by[15]

$$\frac{\langle R_i^2\rangle}{\langle R_i^2\rangle_0} = 1 + \frac{8}{\pi^2}\frac{1}{\nu k_B T}\sigma_{ii}^1 \qquad (17)$$

In a frame whose axes are oriented with the principal axes of the deformed macromolecule, we find from the exact formula (16) that at $\dot{\epsilon}_c$ the distorted coil with 100 springs is stretched to 6.33 times its equilibrium dimension in the maximum stretch direction and is compressed to 0.71 times its equilibrium dimension in the maximum compressional direction. Its dimension is unchanged in the neutral direction. The approximate formula (17) gives similar values—6.26, 0.77, and 1—for these relative dimensions. The results for $N = 25$ are also close to these. Thus the stretched dimension of the coil is considerably larger than the value 1.35 that one obtains from the cylinder model.

We can also compute the degree of stretch as a function of position along the chain:[15]

$$\langle R_k^2\rangle/b^2 = 1 + \frac{1}{3\nu k_B T}\sum_{m=1}^{N}\frac{2}{N}\sin^2\left(\frac{mk\pi}{N+1}\right)\mathrm{tr}\,\sigma^m \qquad (18)$$

where $\langle R_k^2\rangle/b^2$ is the mean square end-to-end length of spring k relative to its equilibrium mean-square length. Again an approximate formula can be derived assuming dominance of the slowest mode:

$$\langle R_k^2\rangle/b^2 = 1 + \frac{1}{3\nu k_B T}\frac{2}{N}\sin\left(\frac{k\pi}{N+1}\right)\mathrm{tr}\,\sigma^1 \qquad (19)$$

From the exact and approximate formulas, one obtains at the critical extension rate $\dot{\epsilon}_c$ the distribution of chain stretching shown for the 100-spring chain in Figure 3. As one would expect, the stretching is concentrated at the center of the molecule. Relative to its equilibrium value the centermost spring of the 100-spring chain is stretched 14%. The centermost spring of the 25-spring chain is stretched 53%; this is about four times as much stretching as is experienced by the centermost spring of the 100-spring chain. A submolecule that is stretched by 53% remains Gaussian if it contains 20 or more Kuhn steps—i.e., has a molecular weight of around 20 000 for polystyrene, for example. Thus if the total molecular weight

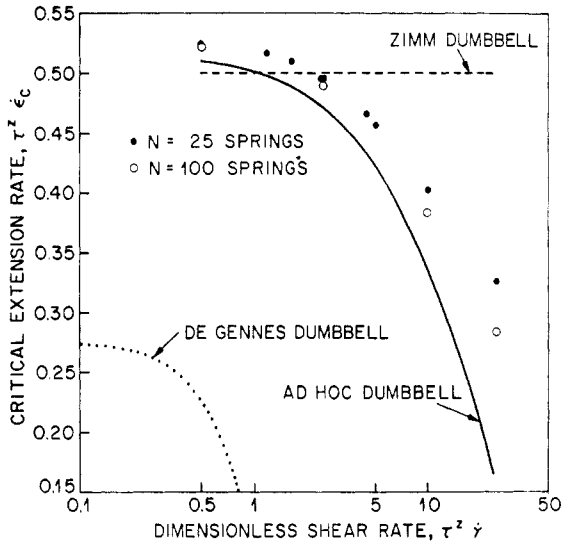

Figure 5. Critical extension rate for a coil–stretch transition as a function of the superposed shear rate for various models.

is more than about 500 000 for polystyrene, the stretching of the centermost portion of the molecule at the coil–stretch transition does not exceed Gaussian limits.

Figure 4 shows the stress invariant $\Delta\sigma$ defined in eq 13 as a function of the extension rate $\dot{\epsilon}$ for $\dot{\gamma}$ = 2, 10, and 40 with 25 and 100 springs. At high levels of stretching, $\Delta\sigma \approx 3\langle R^2\rangle/\langle R^2\rangle_0$; $\Delta\sigma$ is therefore roughly the square of the relative stretch of the chain. The critical extension rate is independent of N, the number of springs, for $N \geq 25$ when $\dot{\gamma}$ is 10 or less. For large $\dot{\gamma}$, however, 25 springs are insufficient to obtain large-N asymptotic results because the distortion of the coil at $\dot{\epsilon}_c$ increases as $\dot{\gamma}$ increases. As we reported in ref 14, the number of springs required to obtain asymptotic results increases as the coil becomes more distorted. Figure 5 plots $\tau^Z\dot{\epsilon}_c$ versus $\tau^Z\dot{\gamma}$ for $N = 25$ and $N = 100$. Here τ^Z is the longest relaxation time in the undistorted (or Zimm) limit. The predictions of the Zimm dumbbell (in which $\tau = \tau^Z$, a constant) and the de Gennes dumbbell model with τ^R/τ^Z large are also plotted for comparison. Note that both the magnitude of $\dot{\epsilon}_c$ and the relative insensitivity of $\dot{\epsilon}_c$ to $\dot{\gamma}$ for the bead–spring calculations at modest $\dot{\gamma}$ are in better agreement with the Zimm dumbbell than with the de Gennes dumbbell! The bead–spring calculations do show a decrease in $\dot{\epsilon}_c$ with increasing

$\dot{\gamma}$, but the decrease exceeds 20% only when $\tau^Z\dot{\gamma}$ reaches 8.0. The ratio $\dot{\epsilon}_c/\dot{\gamma} \approx \rho^{1/2}$ at this point is 0.052. Thus a 20% decrease in $\dot{\epsilon}_c$ is achieved only when $\rho \approx (\dot{\epsilon}_c/\dot{\gamma})^2$ is reduced to 0.003. This result is consistent with the experiments of Dunlap and Leal was found no significant decrease in $\dot{\epsilon}_c = G\rho^{1/2}$ for values of ρ (λ in their notation) as low as 0.019, the lowest value reached in their experiments. The de Gennes dumbbell model (with τ^R/τ^Z large) predicts a 20% reduction in $\dot{\epsilon}_c$ at $\rho \approx (\dot{\epsilon}/\dot{\gamma})^2 = 0.2$.

At values of $\tau^Z\dot{\gamma}$ larger than 8.0, significant decreases in $\dot{\epsilon}_c$ are seen in the bead–spring calculations. James et al.[16] have recently presented experimental data indicating that the critical extension rate for a coil–stretch transition can be significantly decreased if polymer molecules are presheared at a high rate of shear; this is consistent with our calculations.

Note in Figure 5 that the chain with more beads shows a greater departure from Zimm behavior at large shear rates. This probably occurs because the disparity between the Rouse and Zimm relaxation times increases as the number of beads grows; the greater this disparity, the more the effective relaxation time can increase as coil distortion becomes more severe. For chains with only a few beads—10 or so—τ^R and τ^Z are nearly the same; for fewer beads still, τ^R is actually less than τ^Z. Thus for realistic calculations of the effect of chain distortion on hydrodynamic interactions, it is important that the chain contain a large number of beads and springs.

V. Ad Hoc Dumbbell Model

Although the de Gennes dumbbell model agrees with our calculations and with the data of Dunlap and Leal insofar as it predicts a sudden coil–stretch transition at a critical strain rate $\dot{\epsilon}_c$, the predicted dependence of $\dot{\epsilon}_c$ on $\dot{\gamma}$ and the predicted molecular distortion at $\dot{\epsilon}_c$ deviate so markedly from our bead–spring calculations and from the Dunlap–Leal data that for quantitative purposes the Zimm model is actually superior. The apparent source of the error in the de Gennes model is its derivation of the drag coefficient from an assumption of a long cylindrically shaped polymer coil, an assumption that is poor at strain rates up to the coil–stretch transition. Although one might be tempted to abandon the dumbbell model as hopelessly crude for quantitative or even semiquantitative calculations, it is so much simpler to calculate with than the bead–spring chain that we think it worthwhile to attempt to salvage it. Indeed, the complexity of most important polymer flows prohibits the use of any model much more complicated than that of a simple dumbbell in flow simulations.

The major limitation intrinsic to all dumbbell models is that they allow only one mode of relaxation. Since we expect that only the slowest mode will dominate the polymer behavior at the coil–stretch transition, there is hope of fixing the dumbbell model, if a better approximation to the relaxation time τ than that of de Gennes (eq 2) can be found. Suppose we assume with de Gennes that the relaxation time τ depends on $\langle R^2\rangle$ but change the specific form of the dependence. The relaxation of the slowest mode of the bead–spring chain is governed by a tensorial quantity, $2\Lambda_1$, which is the counterpart of the scalar quantity $1/\tau$ in the dumbbell model. Figure 6 plots the 11 and 22 components of $2\Lambda_1$ against tr σ for simple shearing flow. For the dumbbell model, according to eq 10

$$\text{tr } \sigma/\nu kT = \frac{3\langle R^2\rangle}{\langle R^2\rangle_0} - 3 \tag{20}$$

The 11 and 22 components of Λ_1 differ from each other

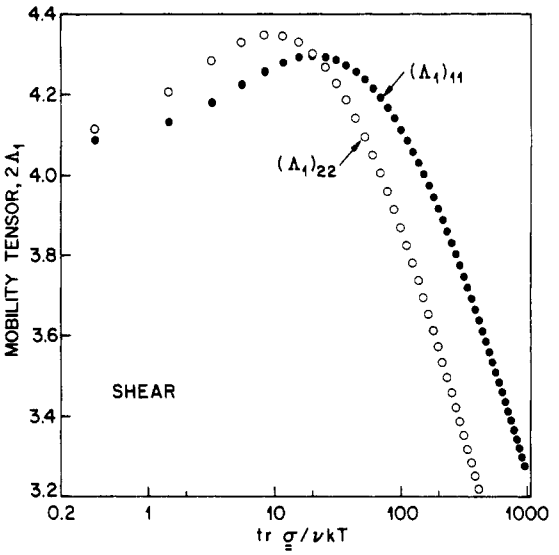

Figure 6. Large components of the mobility tensor as a function of the trace of the stress tensor in shear flow of the bead–spring model with $N = 100$ springs.

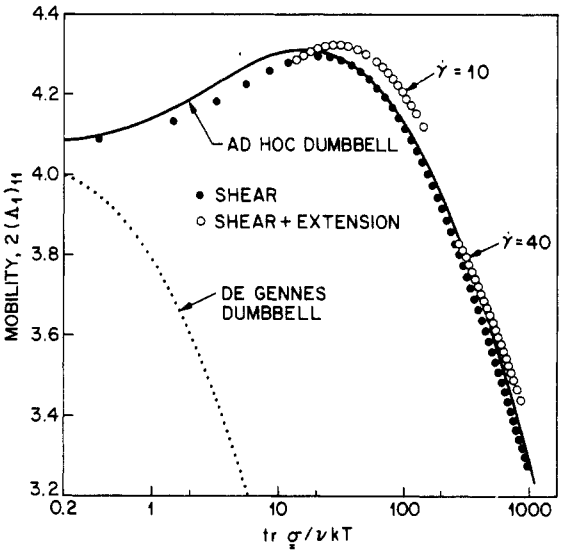

Figure 7. 11 component of the mobility tensor as a function of the trace of the stress tensor in shear and mixed flows for the bead–spring model with $N = 100$ springs. Shown for comparison are the predictions of the de Gennes dumbbell model, eq 4, and the fit given by the ad hoc dumbbell model, eq 17.

by about 10% at high extensions and less at smaller $\langle R^2\rangle$. The 12 component of $2\Lambda_1$ is about 1% as large as the 11 or 22 components. Thus as a rough approximation we may take

$$2\Lambda_1 \approx \frac{1}{\tau}\delta \tag{21}$$

where δ is the unit tensor. We thus neglect the anisotropy in Λ_1. Figure 7 shows the 11 component of $2\Lambda_1$ as a function of tr σ for various combinations of shearing and extension. It is fair to say that $2\Lambda_1$ is roughly a universal function of $\langle R^2\rangle$. Figure 7 also shows, however, that the functional form assumed by de Gennes is a poor approximation to the result obtained from the bead–spring theory. A much better approximation is given by

$$(\Lambda_1)_{11} = \frac{1}{\tau} = \frac{\beta}{1 + \gamma(\text{tr } \sigma/\nu k_B T + 3)^{1/2}} - \frac{\alpha}{(\text{tr } \sigma/\nu k_B T + 3)^{1/2}} \tag{22}$$

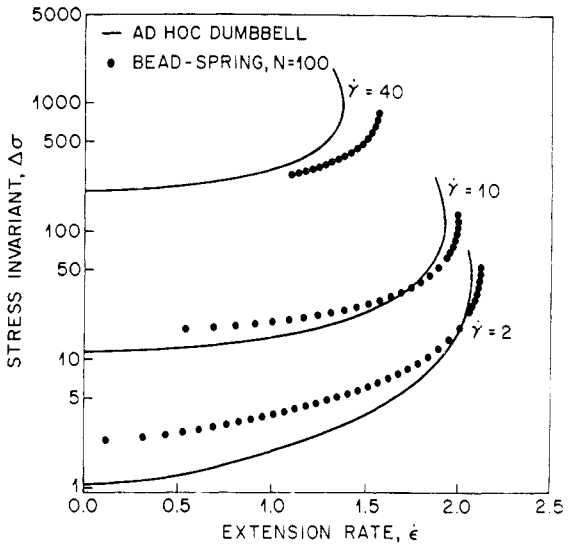

Figure 8. Stress invariant $\Delta\sigma$ versus extension rate for various fixed levels of shear as calculated from the bead–spring model with $N = 100$ springs and from the ad hoc dumbbell model with $\alpha = 1.2$ and $\gamma = 0.015$.

where the condition that $\tau = \tau^Z$ at no distortion, i.e., at tr $\sigma = 0$, gives

$$\beta = \left(\frac{1}{\tau^Z} + \frac{\alpha}{3^{1/2}}\right)(1 + 3^{1/2}\gamma) \tag{23}$$

By adjusting the remaining two parameters α and γ, a good fit of this expression to the dependence of Λ_1 on tr σ in shearing flow is obtained; the fit obtained with $\alpha = 1.2$ and $\gamma = 0.015$ is shown in Figure 7. Note that for large coil distortions, eq 22 and 23 yield $\tau \approx 0.016(3\langle R^2\rangle/\langle R^2\rangle_0)^{1/2}$. The same proportionality, with a much larger coefficient, namely, $\tau \approx 0.14(3\langle R^2\rangle/\langle R^2\rangle_0)^{1/2}$, is obtained with the de Gennes expression.

By use of this ad hoc form for τ ($\langle R^2\rangle$), the predictions of the dumbbell model are compared to those of the bead–spring chain in Figure 8. For any of the dumbbell models, the steady-state stress can be computed from

$$-\tau(\nabla\mathbf{v}^T\cdot\boldsymbol{\sigma} + \boldsymbol{\sigma}\cdot\nabla\mathbf{v}) + \boldsymbol{\sigma} = \nu k_B T\tau(\nabla\mathbf{v}^T + \nabla\mathbf{v}) \tag{24}$$

Rough qualitative agreement between the bead–spring calculations and the ad hoc dumbbell model is obtained, although the agreement becomes poorer as $\dot{\gamma}$ increases. Figure 5 shows that the dependence of $\dot{\epsilon}_c$ on $\dot{\gamma}$ predicted by this ad hoc dumbbell model accords reasonably well with the bead–spring calculations, except at the highest shear rates.

Appendix

The bead–spring calculations for general planar flows were carried out as described in ref 14 for shear flow, with the substitution of the formulas for the tensor $\mathbf{M}$ with

$$M_1^c = \frac{\kappa + 0.5\dot{\gamma}}{(\Lambda_1^c - \kappa)\left(\frac{1}{\Lambda_1^x} + \frac{1}{\Lambda_1^y}\right)(\dot{\gamma} - \Lambda_1^c) + \Lambda_1^y + \Lambda_1^x} \tag{A.1}$$

$$M_1^x = (\dot{\gamma} + \kappa - \Lambda_1^c)M_1^c/\Lambda_1^x \tag{A.2}$$

$$M_1^y = (\kappa - \Lambda_1^c)M_1^c/\Lambda_1^y \tag{A.3}$$

Equation 6 for the velocity gradient tensor was used in the calculations.

References and Notes

(1) Larson, R. G. *Constitutive Equations for Polymer* Melts *and Solutions*; Butterworths: Boston, 1988.
(2) Ferry, J. D. *Viscoelastic Properties of Polymers*, 3rd ed.; Wiley: New York, 1980; pp 183–197, 1980.
(3) de Gennes, P.-G. *J. Chem. Phys.* **1974**, *60*, 5030.
(4) Hinch, E. J. *Proceedings of the Symposium on Polymer Lubrification*; Brest, 1974.
(5) Zimm, B. H. *J. Chem. Phys.* **1956**, *24*, 269.
(6) Rouse, P. E., Jr. *J. Chem. Phys.* **1953**, *21*, 1272.
(7) Noda, I.; Yamada, Y.; Nagasawa, M. *J. Phys. Chem.* **1968**, *72*, 2890.
(8) Bird, R. B.; Curtiss, C. F.; Armstrong, R. C.; Hassager, O. *Dynamics of Polymer Liquids*, 2nd ed.; John Wiley & Sons: New York, 1987; Vol. 2, p 83.
(9) Fuller, G. G.; Leal, L. G. *Rheol. Acta* **1980**, *19*, 580.
(10) Dunlap, P. N.; Leal, L. G. *J. Non-Newt. Fluid Mech.* **1987**, *23*, 5.
(11) Fixman, M. *J. Chem. Phys.* **1966**, *45*, 785, 793.
(12) Öttinger, H. C. *J. Chem. Phys.* **1987**, *86*, 3731.
(13) Magda, J. J.; Larson, R. G.; Mackay, M. E. *J. Chem. Phys.* **1988**, *89*, 2504.
(14) Fixman, M. *Macromolecules* **1981**, *14*, 1710.
(15) King, D. H.; James, D. F. *J. Chem. Phys.* **1983**, *78*, 4743.
(16) James, D. F.; McLean, B. D.; Saringer, J. H. *J. Rheol.* **1987**, *31*, 453.